Supplementary Material for:

Title:

Artificial anion-conducting channelrhodopsins with tuned spectra, modified kinetics and enhanced light sensitivity

Authors:

Jonas Wietek[1], Silvia Rodriguez-Rozada[4#], Janine Tutas[2#], Federico Tenedini[2], Christiane Grimm[1], Thomas G. Oertner[3], Peter Soba[2], Peter Hegemann[1], J. Simon Wiegert[3,4] *

Affiliations:

1 Institute for Biology, Experimental Biophysics, Humboldt-Universität zu Berlin, Invalidenstraße 42, 10115 Berlin, Germany.

2 Research Group Neuronal Patterning and Connectivity, Center for Molecular Neurobiology Hamburg, Falkenried 94, 20251 Hamburg, Germany.

3 Institute for Synaptic Physiology, Center for Molecular Neurobiology Hamburg, Falkenried 94, 20251 Hamburg, Germany.

4 Research Group Synaptic Wiring and Information Processing, Center for Molecular Neurobiology Hamburg, Falkenried 94, 20251 Hamburg, Germany

# equal contribution

* correspondence to: simon.wiegert@zmnh.uni-hamburg.de

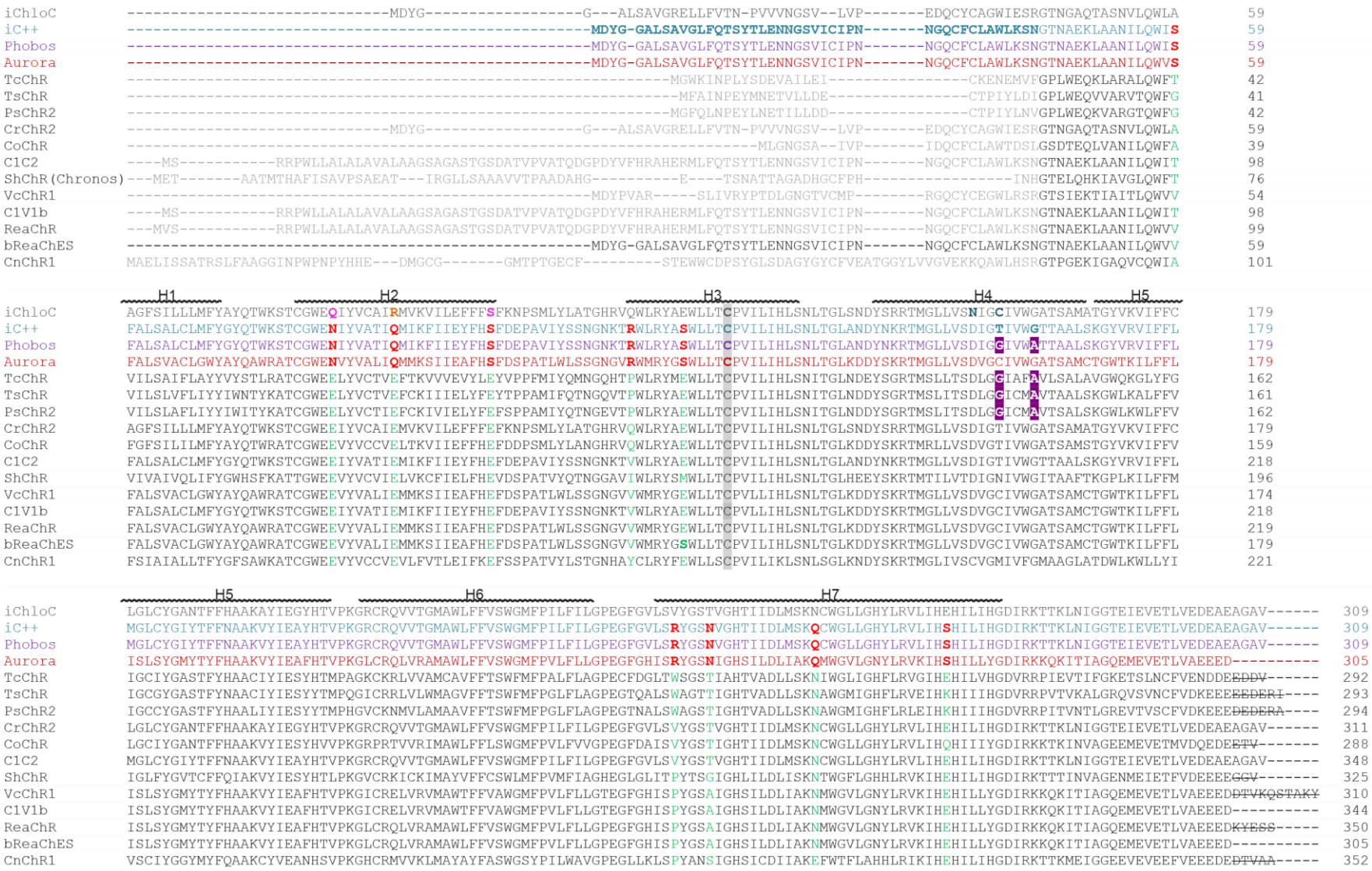

Figure S1: Sequence comparison of aACRs and CCRs. Amino acid sequence alignment [1-3] of iChloC (dark gray), iC++ (dark turquoise), Phobos (deep purple), Aurora (dark red) and all cation-conducting ChRs (CCRs) mutated in this study. Mutations yielding the four ACRs are indicated with bold red letters and homologous positions in CCRs are shown in green. In addition, the E90R (bold orange) as well as E83Q and E101S (bold pink) mutations are highlighted in the iChloC sequence. C128, which was mutated to A to generate SFO-ACRs is highlighted in gray. T159G and G163A mutations in blue-shifted opsins are highlighted in purple. The N-termini replaced for the N-terminus of iC++ (dark bold turquoise) are shown in gray. Please note that the Aurora sequence is identical to bReachES [4] except for the introduced mutations. Crossed amino acids where left out for ic++ based approach.

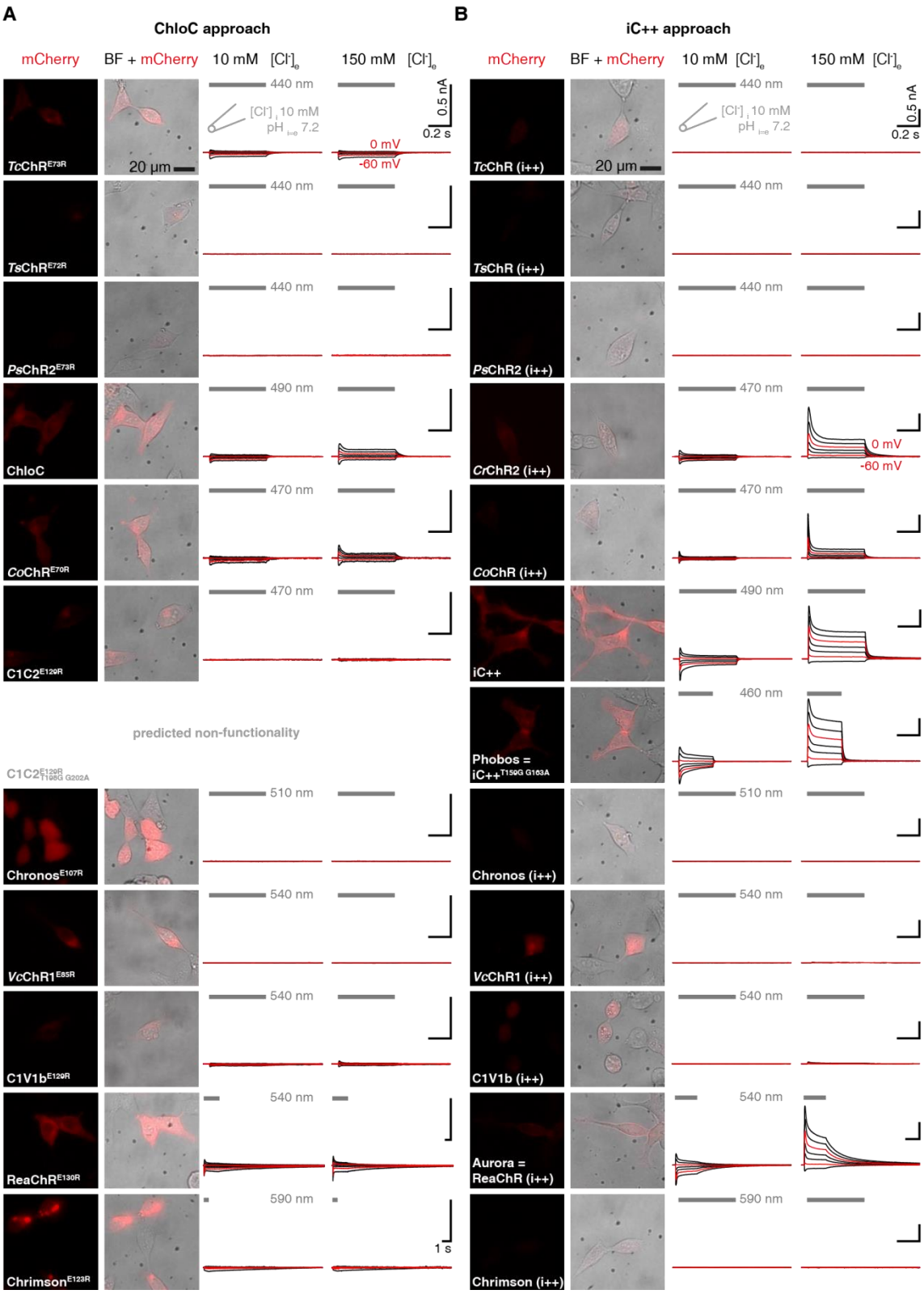

Figure S2: Screening results of the conversion approaches. Summary of converted CCRs tested in this study. Epifluorescence images show localization of converted CCRs labeled by mCherry in HEK cells. Corresponding brightfield (BF) images show HEK cell morphology. Photocurrents at holding potentials ranging from -80 to +40 mV (20 mV increments) in low (10 mM, left) or high (150 mM, right) extracellular chloride. The ChloC-strategy is shown in (**A**), the iC++ approach is shown in (**B**). Parental CCRs with their mutations are indicated for all constructs. For CCR abbreviations please refer to the main text.

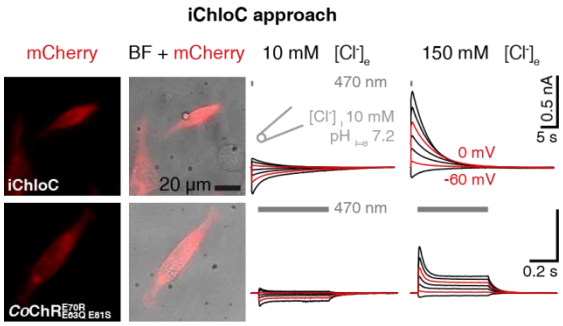

Figure S3: Characterization of *Cr*ChR2 and *Co*ChR converted with the iChloC approach. Epifluorescence images show localization of converted CCRs labeled by mCherry in HEK cells. Corresponding brightfield (BF) images show HEK cell morphology. Photocurrents at holding potentials ranging from -80 to +40 mV (20 mV increments) in low (10 mM, left) or high (150 mM, right) extracellular chloride.

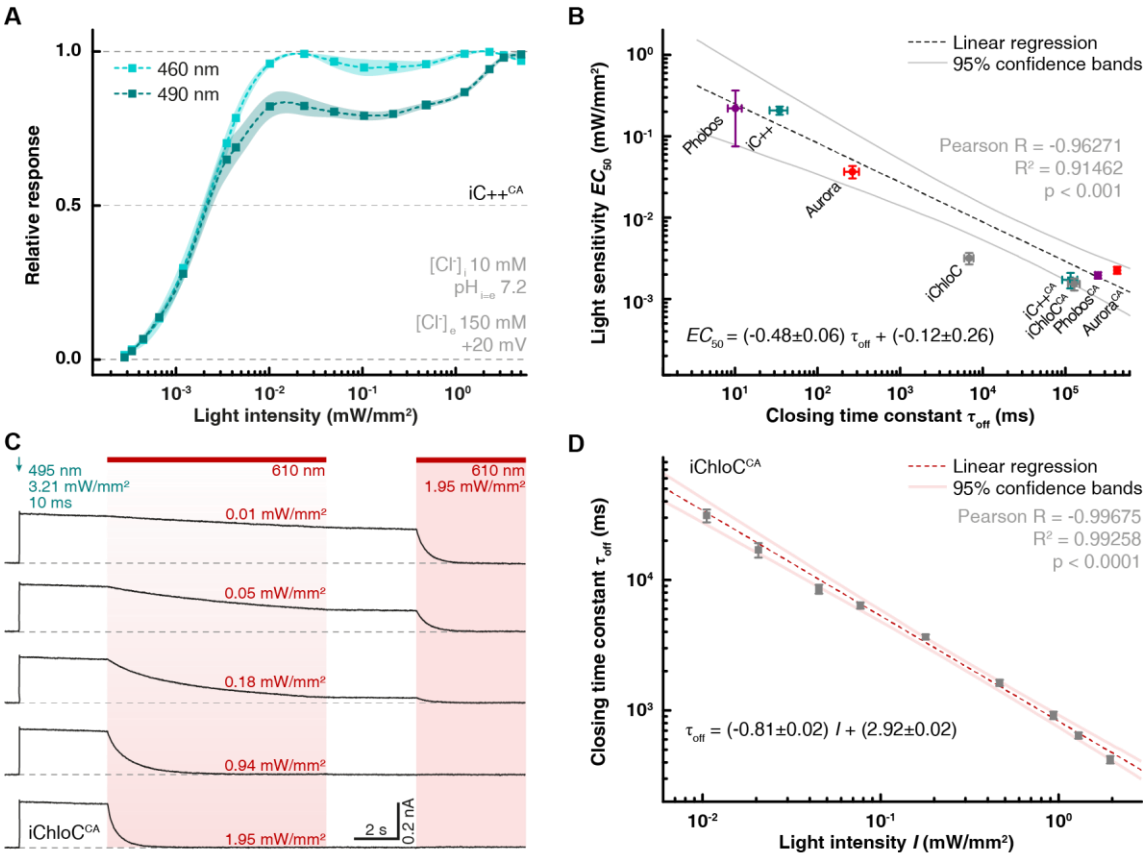

Figure S4: Biophysical properties of step-function-aACRs. (**A**) Light titration of iC++^{CA} termed SwichR++ in, [5] shows reduced partial inactivation for 460 nm (n = 3) compared to activation with 490 nm (n = 6). (**B**) Light sensitivity vs. closing time constant of aACR variants linearly correlates except for iChloC that shows a higher sensitivity compared to other aACRs with respect to its closing time constant. Fitting statistics are listed in the figure panel. (**C** and **D**) Dependence of accelerated iChloC^{CA} channel closing on light dose. (C) Example traces from a single experiment. (D) Data from multiple experiments (n = 6 HEK cells) show a linear relationship between closing speed and light intensity. Fitting statistics are listed in the figure panel.

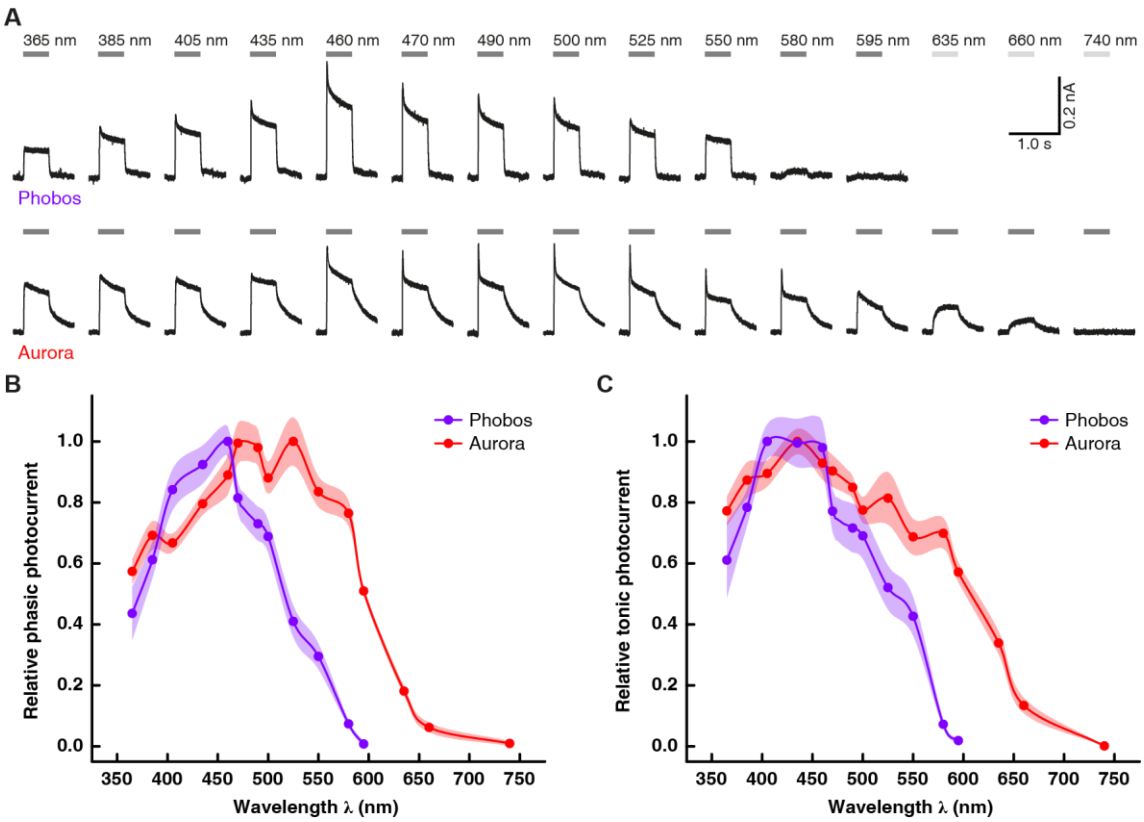

Figure S5: Action spectra of Phobos and Aurora photocurrents in neurons. (**A**) Example traces of Phobos (top row) or Aurora photocurrents (bottom row) evoked at indicated wavelengths (500 ms, 10 mW/mm^2) in CA1 pyramidal neurons clamped at -50 mV. (**B**) and (**C**) Action spectra of normalized peak (B) and tonic (C) Phobos and Aurora photocurrents.

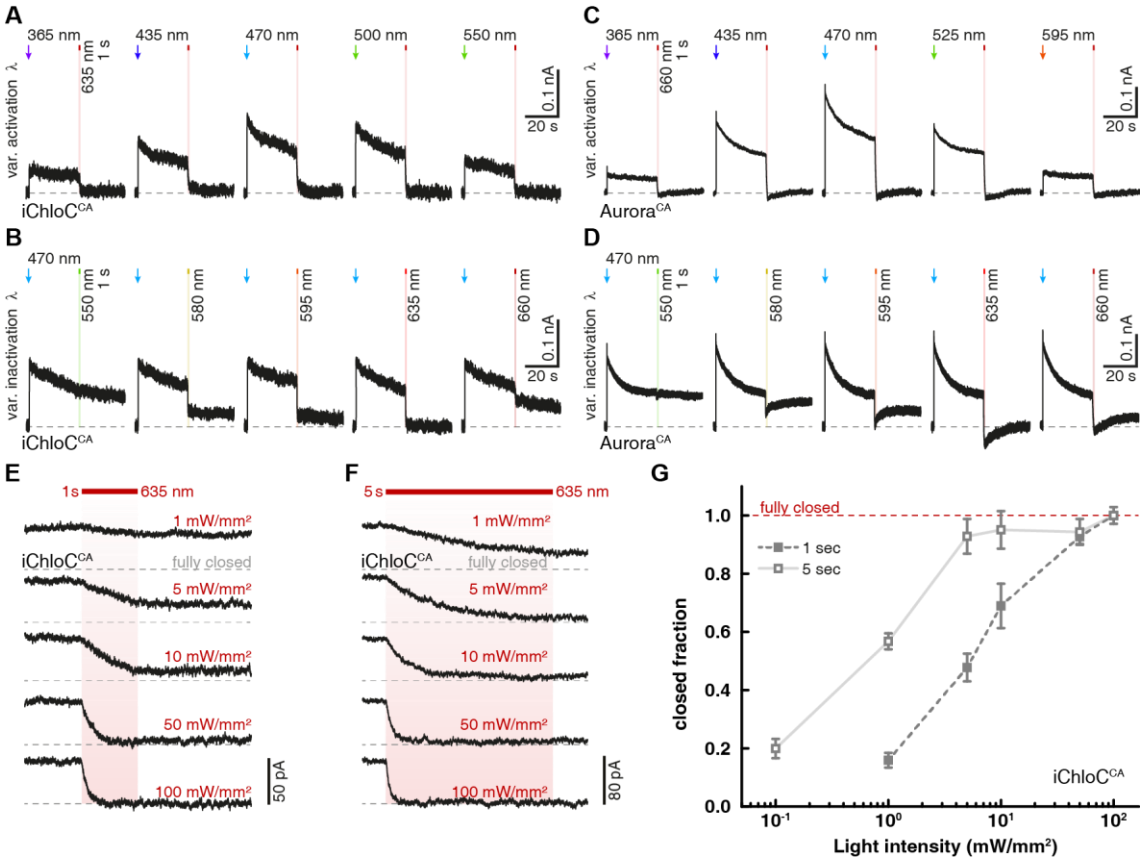

Figure S6: Light-dependent activation and inactivation of SFO-aACRs in CA1 pyramidal neurons. (**A**) Representative recordings of photocurrents in an iChloC^{CA}-Citrine expressing CA1 cell. Photocurrents were evoked with different activation wavelengths and shutoff with 635 nm light. (**B**) Photocurrent traces in the same cell evoked with 470 nm light and shutoff with at indicated wavelengths (10 mW/mm^2). (**C**) Representative recordings of photocurrents in an Aurora^{CA}-Citrine expressing CA1 cell. Photocurrents were evoked with different activation wavelengths and shutoff with 660 nm light. (**D**) Photocurrent traces in the same cell evoked with 470 nm light and shutoff with at indicated wavelengths (10 mW/mm^2). (**E**) and (**F**) Example recordings showing light-accelerated channel closing of iChloC^{CA}-Citrine in CA1 pyramidal neurons. Channel closing was accelerated by illumination with 635 nm light at indicated powers for 1s (E) or 5s (F). (**G**) Quantification of experiments shown in (E) and (F). Full channel closing could be achieved with 5 mW/mm^2 over 5 sec or 50 mW/mm^2 over 1 sec (n = 5 neurons in 5 slice cultures). Averages are shown as rectangular symbols with SEM.

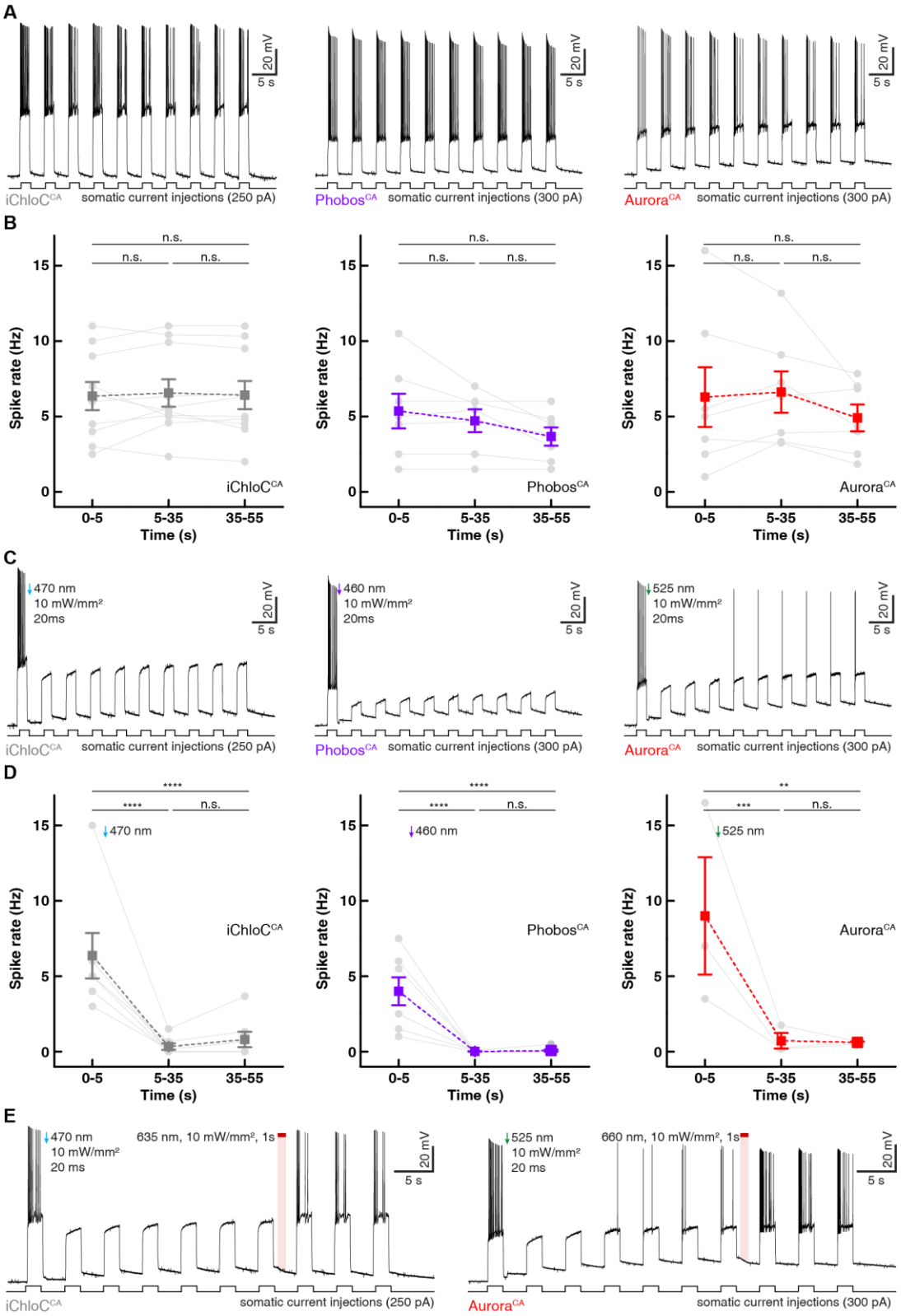

Figure S7: Performance of SFO-aACRs in CA1 pyramidal neurons. (**A**) Membrane voltage traces show reliable depolarization-induced action potential firing of Phobos^{CA}-Citrine, iChloC^{CA}-Citrine and Aurora^{CA}-Citrine expressing CA1 pyramidal neurons in the absence of light. (**B**) Quantification of the spike rate during current injection at indicated time intervals (n = 10, 7, 5 for iChloC^{CA}, Phobos^{CA} and Aurora^{CA}, respectively, repeated measures one-way ANOVA followed by Tukey's multiple comparisons test). (**C**) Membrane voltage traces show inhibition of depolarization-induced action potential firing of Phobos^{CA}-Citrine, iChloC^{CA}-Citrine and Aurora^{CA}-Citrine expressing CA1 pyramidal neurons in response to a 20 ms light pulse. (**D**) Quantification of the spike rate during current injection at indicated time intervals before (0-5 s) and after the light pulse (5-35 and 35-55 s). n = 7, 7, 3 for iChloC^{CA}, Phobos^{CA} and Aurora^{CA}, respectively, **: $p < 0.01$, ***: $p < 0.001$, ****: $p < 0.0001$, repeated measures one-way ANOVA followed by Tukey's multiple comparisons test). (**E**) Membrane voltage traces showing reversible suppression of depolarization-induced spiking by photoswitching iChloC^{CA} (left) and Aurora^{CA} (right) between open and closed state. Light gray symbols indicate individual experiments. Averages are shown as rectangular symbols with SEM.

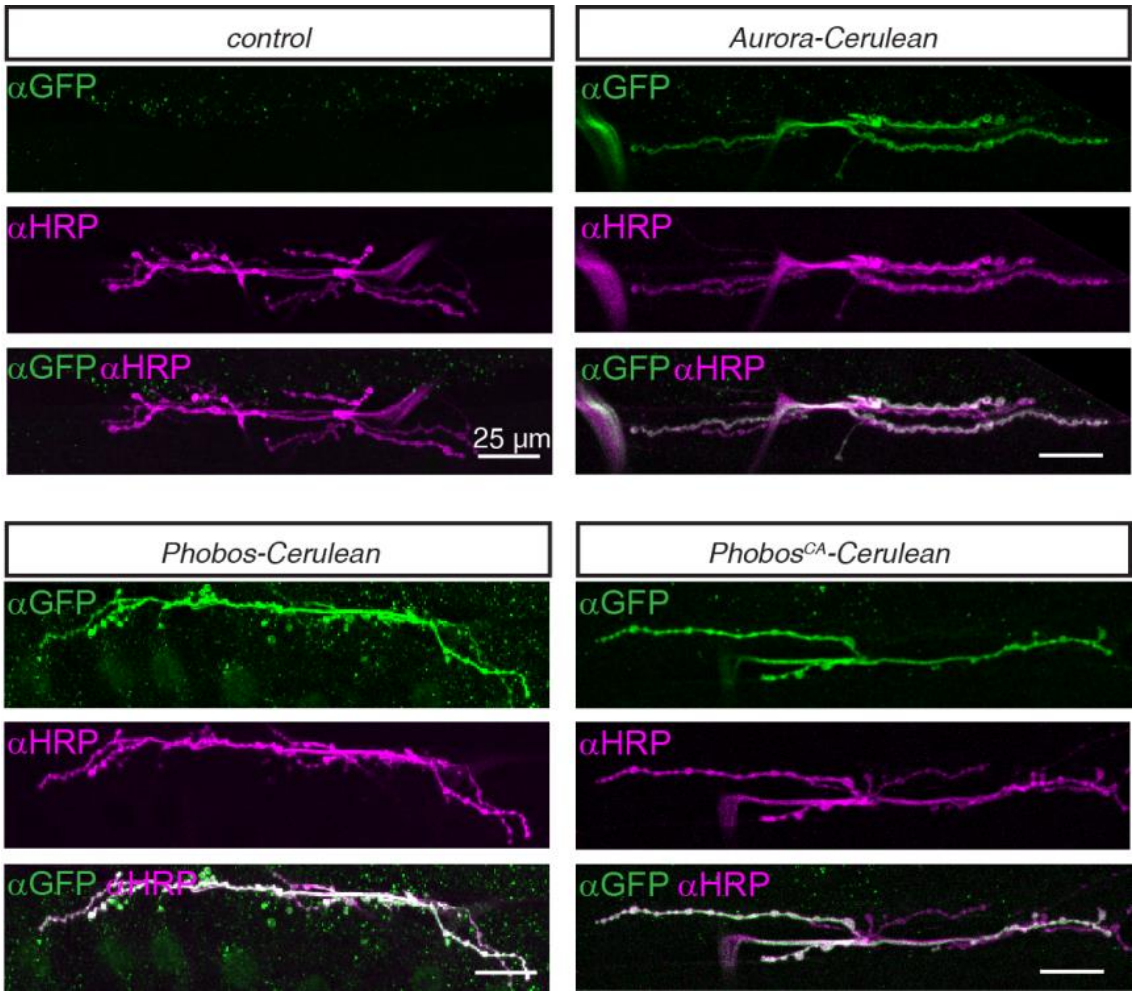

Figure S8: Expression and localization of Aurora, Phobos and Phobos^{CA}. Representative images of neuromuscular junctions (NMJs) at muscle 6/7 for control, Aurora-Cerulean, Phobos-Cerulean and Phobos^{CA}-Cerulean expressing motor neurons (*ok371-Gal4*). aACR expression and localization was visualized by anti-GFP immunohistochemistry together with a neuronal surface marker anti-HRP (horseradish peroxidase). aACRs did not obviously affect NMJ morphology and showed extensive colocalization with αHRP at the neuronal cell surface. Scale bar: 25µm.

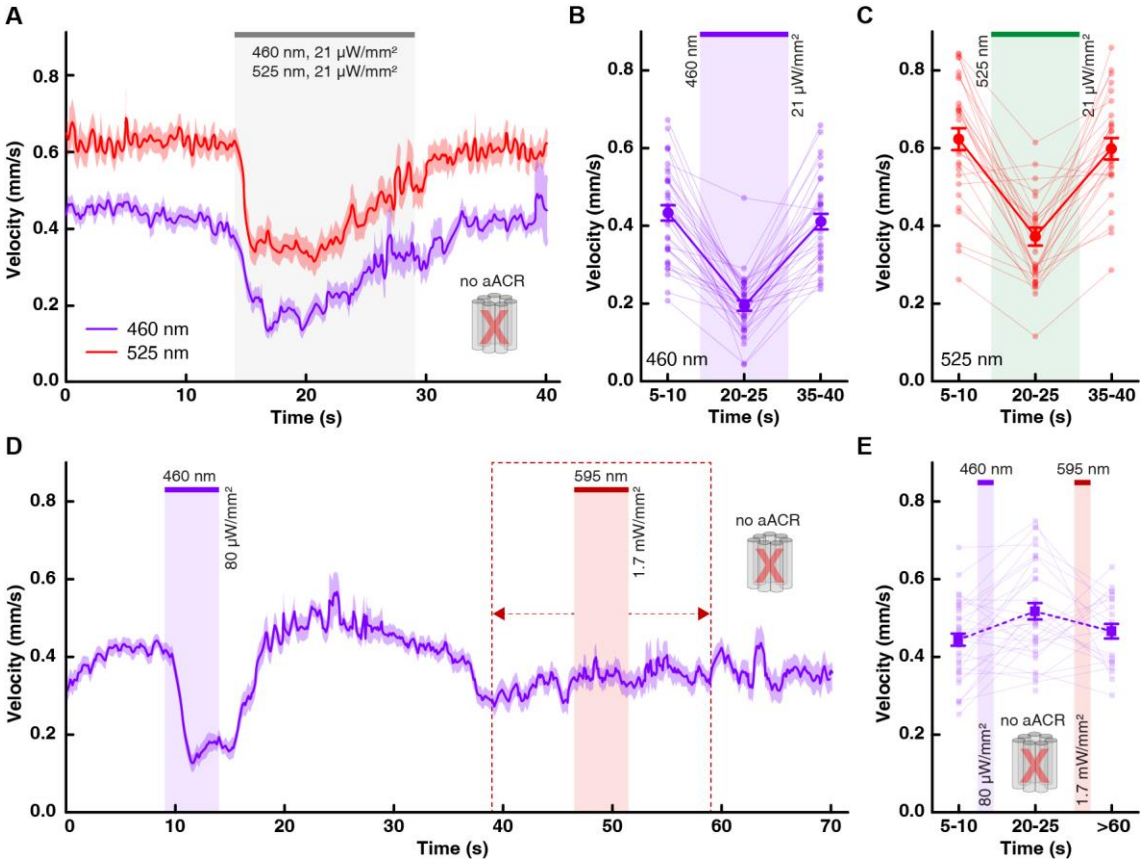

Figure S9: Innate responses to light during Drosophila locomotion behavior. (**A**) Larval velocity over time is plotted for control animals (w^-), with 15 s of light stimulation with 460 nm or 525 nm. (n = 37 animals for 460 nm and n= 34 for 525 nm, mean ± SEM). (**B** and **C**) Averaged velocity from experiments in (A) analyzed in 5 s time bins before (5-10 s), during (20-25 s) and after (35-40 s) exposure to the indicated light intensity and wavelength (n = 37 for 460 nm in B and n = 34 for 525 nm in C, mean ± SEM). (**D**) Velocity of control animals (w^-) over time under the same conditions of light exposure as Phobos^{CA} using 5 s of 460 nm light exposure and 5 s of 595 nm light (n = 38, mean ± SEM). All animals on an agar plate were sequentially illuminated (5 s each) for channel closing during the time period indicated by the dashed box. (**E**) Averaged velocity from experiments in (D) analyzed in 5 s time bins before (5 – 10 s), during (20 – 25 s) and after (>60 s) exposure to the indicated light intensity and wavelength (n = 37, mean ± SEM).

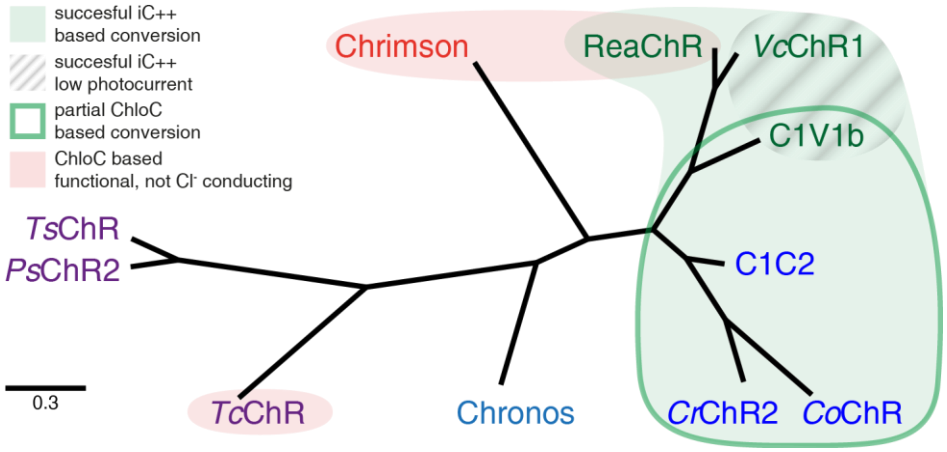

Figure S10: Phylogenetic tree of converted CCRs. A phylogenetic tree was generated for all CCRs listed in Figure S1 using phylogeny.fr [6]. N-terminal amino acids were excluded up to the position where the N-termini were replaced for the chimeric C2C1 N-terminus of iC++. Successfully converted CCRs cluster in the two right clades. CCR names are color coded according to their spectral absorption.

Table S1. Neuronal membrane parameters in the dark.

	wt (n = 10)	SD	Aurora (n = 9)	SD	Phobos (n = 7)	SD	Aurora^{CA} (n = 11)	SD	Phobos^{CA} (n = 8)	SD	iChloC^{CA} (n = 9)	SD	ANOVA
AP threshold (mV)	-50.70	2.47	-46.45	4.17	-44.99	3.73	-42.79	8.06	-47.48	4.29	-46.15	4.89	**
AP peak (mV)	35.82	2.94	32.31	2.47	34.49	3.08	35.82	4.15	32.71	2.23	35.98	4.68	n.s.
AP amplitude (mV)	114.05	5.37	107.57	3.88	108.31	4.71	107.02	7.59	112.14	4.35	115.32	3.65	*
n AP's	13.70	2.93	17.00	2.26	11.29	2.19	8.45	5.25	13.50	3.81	15.33	3.77	*
E_{Rest} (mV)	-78.23	4.61	-75.26	2.86	-73.82	3.35	-72.95	6.22	-79.43	3.74	-79.34	3.97	*
R_m (Mohm)	152.17	67.28	143.40	66.03	147.76	66.62	71.93	18.24	124.25	20.64	172.09	42.10	*

Electrical parameters of untransfected (wt) pyramidal CA1 neurons and neurons expressing the indicated aACR-Citrine fusion construct together with mCerulean. Action potentials (APs) were evoked by a square current pulse (500 ms, 500 pA) in current clamp mode. Threshold, peak voltage and amplitude were calculated for the first AP. Membrane resistance (R_m) was measured in voltage clamp mode in response to a square voltage pulse (− 5 mV, 100 ms). E_{rest} = resting membrane potential, S.D. = standard deviation. Right column indicates p-values from one-way ANOVA for each parameter. n.s. no significant differences, * P < 0.05. Gray field marks value significantly different to non-transfected (wt) neurons. All measurements were liquid junction potential corrected.

References

1 McWilliam, H. *et al.* Analysis Tool Web Services from the EMBL-EBI. *Nucleic Acids Res* **41**, W597-600, doi:10.1093/nar/gkt376 (2013).

2 Li, W. *et al.* The EMBL-EBI bioinformatics web and programmatic tools framework. *Nucleic Acids Res* **43**, W580-584, doi:10.1093/nar/gkv279 (2015).

3 Sievers, F. *et al.* Fast, scalable generation of high-quality protein multiple sequence alignments using Clustal Omega. *Mol Syst Biol* **7**, 539, doi:10.1038/msb.2011.75 (2011).

4 Rajasethupathy, P. *et al.* Projections from neocortex mediate top-down control of memory retrieval. *Nature* **526**, 653-659, doi:10.1038/nature15389 (2015).

5 Berndt, A. *et al.* Structural foundations of optogenetics: Determinants of channelrhodopsin ion selectivity. *Proc Natl Acad Sci U S A* **113**, 822-829, doi:10.1073/pnas.1523341113 (2016).

6 Dereeper, A. *et al.* Phylogeny.fr: robust phylogenetic analysis for the non-specialist. *Nucleic Acids Res* **36**, W465-469, doi:10.1093/nar/gkn180 (2008).